

**PULSE HEIGHT TALLY RESPONSE EXPANSION
METHOD FOR APPLICATION IN DETECTOR
PROBLEMS**

A Thesis
Presented to
The Academic Faculty

by

Travis J. Zipperer

In Partial Fulfillment
of the Requirements for the Degree
Masters of Science in
Nuclear Engineering

Georgia Institute of Technology
August 2011

**PULSE HEIGHT TALLY RESPONSE EXPANSION
METHOD FOR APPLICATION IN DETECTOR
PROBLEMS**

Approved by:

Dr. Farzad Rahnema, Advisor
Nuclear and Radiological Engineering
Georgia Institute of Technology

Dr. Dingkang Zhang
Nuclear and Radiological Engineering
Georgia Institute of Technology

Dr. Glenn Sjoden
Nuclear and Radiological Engineering
Georgia Institute of Technology

Date Approved: 17 June 2011

ACKNOWLEDGEMENTS

There are several who I would like to thank for their assistance. I would like to thank my advisor, Dr. Rahnema for his guidance, instruction and support, Dr. Zhang for his tireless patience in answering and assisting me in my many questions and issues, and Dr. Sjoden for taking part in the review of my thesis. Additionally, I would like to thank Robert Hayward, Justin Pounders, Jack Zhang, Kevin Connolly, and Steven Douglass for their assistance in various areas of my research.

I cannot express enough gratitude and appreciation for my girlfriend, Damaris Rodriguez, for her love, encouragement, and support in all aspects of my life. I am truly blessed to have her.

Last but not least, I would like to thank God for all that He has given to me. Without Him, none of this would have been possible.

TABLE OF CONTENTS

ACKNOWLEDGEMENTS	iii
LIST OF TABLES	v
LIST OF FIGURES	vi
SUMMARY	viii
I INTRODUCTION	1
II BACKGROUND	3
III METHOD	5
3.1 Monte Carlo Estimators	5
3.2 Expansion Method	6
3.3 Incident Flux Approximation	9
3.4 Implementation of the Method	10
IV RESULTS	13
4.1 Method Verification	13
4.1.1 Multigroup Flux Approximations	14
4.1.2 Continuous Flux Approximations	15
4.1.3 Pulse Height Tally Solutions	18
4.2 Accuracy and Efficiency	24
V CONCLUSION, RECOMMENDATION, AND FUTURE WORK	26
APPENDIX A — FLUX ENERGY BINS	28
REFERENCES	29

LIST OF TABLES

1	2-Norms of U-235 flux distribution for B-spline approximations	18
2	Percent mean weighted errors of response expansion method for pulse height tallies	25
3	Computation times for pulse height tally solutions for MCNP5 and the response expansion method	25
4	Energy bins for flux spectrums	28

LIST OF FIGURES

1	1 st (top), 2 nd (middle) and 3 rd (bottom) order B-spline basis on the interval [0,1] with 5 uniform subintervals.	10
2	Diagram of the detector with a photon flux incident on one of the 13.5x13.5 cm detector faces. The detector is composed of a CsI(Na) crystal.	13
3	Incident flux from an air cargo	14
4	Incident flux from a third-density water cargo	15
5	The 1 st , 2 nd and 3 rd order B-spline approximations of the U-235 prompt fission gamma distribution compared to the exact solution of the distribution.	16
6	The 2 nd and 3 rd order B-spline approximations, with additional knots at 0.3 MeV and 1.0 MeV, of the U-235 prompt fission gamma distribution compared to the exact solution of the distribution.	17
7	Comparison of MCNP5's and the response expansion method's pulse height tally associated with the incident flux from the air cargo. . . .	19
8	Comparison of MCNP5's and the response expansion method's pulse height tally associated with the incident flux from the third-density water cargo.	20
9	Comparison of the pulse height tally associated with the U-235 distribution from MCNP5 and the pulse height tally from the response expansion method using the 1 st order B-spline approximation of the U-235 distribution.	21
10	Comparison of the pulse height tally associated with the U-235 distribution from MCNP5 and the pulse height tally from the response expansion method using the 2 nd order B-spline approximation of the U-235 distribution.	22
11	Comparison of the pulse height tally associated with the U-235 distribution from MCNP5 and the pulse height tally from the response expansion method using the 3 rd order B-spline approximation of the U-235 distribution.	22
12	Comparison of the pulse height tally associated with the U-235 distribution from MCNP5 and the pulse height tally from the response expansion method using the 2 nd order B-spline approximation (with additional knots) of the U-235 distribution.	23

13 Comparison of the pulse height tally associated with the U-235 distribution from MCNP5 and the pulse height tally from the response expansion method using the 3rd order B-spline approximation (with additional knots) of the U-235 distribution. 24

SUMMARY

A pulse height tally response expansion (PHRE) method is developed for detectors. By expanding the incident flux at the detector window/surface, a set of response functions is constructed via Monte Carlo estimators for pulse height tallies. B-spline functions are selected to perform the expansion of the response functions as well as for the expansion of the incident flux in photon energy. The method is verified for several incident flux spectra on a CsI(Na) detector. Results are compared to the solutions generated using direct Monte Carlo calculations. It is found that the method is several orders faster than MCNP5 while maintaining paralleled accuracy.

CHAPTER I

INTRODUCTION

Interrogation of cargo containers falls within the category of large radiation detector problems in which numerical radiation transport calculations are needed to identify clandestine materials. Cargo containers may carry numerous amounts and types of cargos that, in turn, may be used to shield clandestine nuclear materials. For each of the various cargos, a new and distinct Monte Carlo simulation would be required. Due to the large number of required simulations in combination with the size of the cargo containers and the level of attenuation within the cargo, direct use of Monte Carlo methods is not a viable means for modeling these systems.

Current research in interrogation problems has spurred the use of hybrid methods to accelerate simulations for these types of problems. Hybrid methods allow the implementation of multiple approaches within one problem by breaking down a problem into various facets. Each facet is then paired with the best-suited method and modeled accordingly. For example, interrogation problems can be separated into two components: the field region (e.g., cargo container), and the detector. The field region and detector can then be modeled respectively using deterministic and Monte Carlo methods [1].

Though the hybrid method provides faster solutions than previous methods, a more efficient method would involve further reduction of the need for Monte Carlo methods. For example, in cargo interrogation problems where the cargo container changes for nearly every problem, the detector can remain the same. Having to perform Monte Carlo calculations for the same detector for each cargo scenario is computationally inefficient. In this study, a method is introduced that accelerates the

computation of detector responses for multiple cargo scenarios in which the detector remains the same. The new method utilizes response functions generated using Monte Carlo methods. These functions are dependent only on the geometry and composition of the detector and, therefore, can be precomputed as the method's library. Once the incident flux is known, this library is used to construct the detector's response (pulse height tally) with accuracy parallel to Monte Carlo methods but significantly more efficiently.

A brief background and the application of the new method are given in chapter II. The new method is described in chapter III. The method's accuracy and efficiency are presented in the results (chapter IV). Finally, conclusions, recommendations, and future work are found in chapter V.

CHAPTER II

BACKGROUND

Monte Carlo methods can simulate a detector's response through pulse height tallies. Pulse height tallies provide the total energy deposited by each particle and the respective progeny within the detector. To obtain the energy deposition of each particle, detailed information on the history of each individual particle within the detector is needed. For this reason, simulation of detector responses has been, for the most part, limited to Monte Carlo methods. Only recently a deterministic method has been introduced to simulate detector responses. However, it has only been demonstrated for one-dimensional cases [2].

When attempting to compute detector responses for large detector problems such as the interrogation of cargo containers, direct Monte Carlo calculations of the pulse height tally can require large computation times. Consequently, direct Monte Carlo calculations are not a practical means to compute such problems. Hybrid methods have been introduced recently to reduce the use of Monte Carlo calculations in an effort to accelerate the computations of interrogation type problems [1]. Where the detector is modeled using Monte Carlo methods, the typically faster deterministic methods are used to model the remainder of the problem or the field region (e.g., cargo container). Unlike the detector, modeling of the field region does not require the detailed history of the individual particles, thus a deterministic method can be applied [1]. To compute the pulse height tally using a hybrid method, the deterministic method must first be used to compute the angular flux of the field region on the boundaries of the detector. Then, these angular fluxes are inputted into the Monte Carlo model of the detector that, in turn, computes the pulse height tally.

Commonly for interrogation problems, Monte Carlo simulations are repeatedly performed in the detector with various incident angular fluxes resulting from the changes within the field region. Therefore, the only change in these simulations is the detector boundary conditions (i.e., incident flux). In these circumstances, the geometry and composition of the detector remain the same. Within this study, the lack of change in the geometry and composition of the detector is taken advantage of in order to improve the efficiency of the Monte Carlo calculations of the detector response. The basis for the new method is the incident flux response expansion method (IFRE) developed for reactor core transport problems by Mosher and Rahnema [3]. The IFRE method approximates the solution (angular flux) of the neutron transport equation for a mesh by equating it to a set of truncated expansions. These expansions are composed of a set of response functions and the corresponding coefficients that depend on the mesh boundary incident fluxes. The response functions are solutions to the transport equation in each unique mesh with boundary conditions defined as a set of known (pre-selected) orthogonal basis functions (e.g., Legendre polynomials). The response functions depend only on the geometry and composition of the mesh (e.g., fuel assembly type) and therefore can be precomputed as the library for the method. Adapting the IFRE method to detectors and using Monte Carlo simulations to generate the detector response functions, pulse height tally calculations for detectors can then be computed significantly more efficiently, as described in the following sections.

CHAPTER III

METHOD

This chapter describes the pulse height tally response expansion (PHRE) method. The general form of the method is developed from the Monte Carlo estimators for pulse height tallies via expansion of the incident flux. B-splines are introduced as the selected choice of bases for the expansions. Finally, the implementation of the energy dependent method utilizing B-splines is discussed.

3.1 Monte Carlo Estimators

Photon interactions within a detector bring about the release of electrons or photons resulting from pair production, Compton scatter, photoelectric effects, and electron-positron annihilation. For the Monte Carlo estimator of a pulse height tally, these interactions can be bundled into a function, denoted by g which represents the probability that a particle and its progeny will deposit a certain amount of energy in the detector. On a seven-dimensional phase space represented by space (\vec{r}), angle ($\hat{\Omega}$), energy (E), and time (t) with $\gamma = (\vec{r}, \hat{\Omega}, E, t)$, the function g for a given particle is given by $g(\epsilon, \gamma)$ where ϵ denotes the energy deposited by a particle and its progeny. The function $g(\epsilon, \gamma)$ represents the probability that a particle at location \vec{r} , angle $\hat{\Omega}$, energy E , and time t will deposit ϵ in energy within the detector. From $g(\epsilon, \gamma)$ and a volumetric uncollided flux, $\Psi(\gamma)$, the pulse height tally for the detector can be represented as a function of energy deposition

$$r(\epsilon) = \int_{\Gamma} g(\epsilon, \gamma) \Psi(\gamma) d\gamma, \quad (1)$$

where Γ represents the domain of integration that encompasses the seven-dimensional phase.

The integral nature of Monte Carlo estimators prevents direct acquirement of a continuous function of Equation (1). Instead, a binned estimator is computed. First, the energy deposition phase space is restricted to the finite interval $[a, b]$ with the interval represented by $N + 1$ bins,

$$a = \epsilon_0 < \epsilon_1 < \dots < \epsilon_N = b. \quad (2)$$

Then, integrating the function $r(\epsilon)$ over a given bin, the binned estimator for the pulse height tally can be represented as,

$$r_i = \int_{\epsilon_{i-1}}^{\epsilon_i} r(\epsilon) d\epsilon, \quad i = 1, 2, \dots, N. \quad (3)$$

A simple and common representation of the function $r(\epsilon)$ is a histogram representation, which assumes $r(\epsilon)$ to be piece-wise constant. The histogram approximation can be given by

$$r_H(\epsilon) = \sum_{i=1}^N \frac{r_i}{\epsilon_i - \epsilon_{i-1}} \chi_{[\epsilon_{i-1}, \epsilon_i]}, \quad (4)$$

where

$$\chi_{[\epsilon_{i-1}, \epsilon_i]} = \begin{cases} 1, & \epsilon_{i-1} \leq \epsilon \leq \epsilon_i \\ 0, & \text{otherwise} \end{cases}. \quad (5)$$

3.2 Expansion Method

For a detector of volume V , the volumetric uncollided flux, $\Psi(\gamma)$, satisfies the following transport equation,

$$\hat{\Omega} \cdot \nabla \Psi(\gamma) + \sigma \Psi(\gamma) = 0, \quad \vec{r} \in V, \quad (6)$$

with the boundary condition defined as the flux incident on the detector,

$$\Psi(\gamma^+) = \varphi(\gamma^+), \quad \vec{r} \in \partial V. \quad (7)$$

The macroscopic cross section, σ , depends on position and energy. The superscript ”+” represents the incoming direction on the surface, $\vec{r} \in \partial V$. The incident flux φ is

assumed to be known. Any change in the incident flux requires the recomputation of this transport equation. By representing the incident flux as an expansion function, a set of transport equations can be solved that are independent of the shape of the incident flux.

Let F_j , where $j = 1, 2, \dots$, represent a complete set of arbitrary expansion (of not necessarily orthogonal) basis functions on γ_s^+ , where the subscript "s" represents one of the surfaces of the detector. The incident flux on the detector surfaces can be represented by the following equation,

$$\varphi(\gamma^+) = \sum_{j=1}^{\infty} \sum_s \alpha_{j,s} F_j(\gamma_s^+), \quad (8)$$

where the set of coefficients $\alpha_s = \{\alpha_{1,s}, \alpha_{2,s}, \dots, \alpha_{j,s}, \dots\}$ for surface s is computed by the pseudoinverse [4]

$$\alpha_s = (F^* F)^{-1} F^* \varphi(\gamma^+). \quad (9)$$

Instead of solving the transport equation using the incident flux as the boundary conditions, it is solved with boundary conditions defined as expansion basis functions. The transport equation now takes the form

$$\hat{\Omega} \cdot \nabla H_{j,s}(\gamma) + \sigma H_{j,s}(\gamma) = 0, \quad \vec{r} \in V, \quad (10)$$

with the boundary condition

$$H_{j,s}(\gamma^+) = F_j(\gamma_s^+), \quad \vec{r} \in \partial V. \quad (11)$$

The volumetric uncollided flux of Equations (6) and (7) can now be represented by

$$\Psi(\gamma) = \sum_{j=1}^{\infty} \sum_s \alpha_{j,s} H_{j,s}(\gamma). \quad (12)$$

Replacing the volumetric uncollided flux of Equation (1) with the form provided in Equation (12), the pulse height tally becomes

$$r(\epsilon) = \sum_{j=1}^{\infty} \sum_s \alpha_{j,s} R_{j,s}(\epsilon), \quad (13)$$

where

$$R_{j,s}(\epsilon) = \int_{\Gamma} g(\epsilon, \gamma) H_{j,s}(\gamma) \partial\gamma. \quad (14)$$

The response function R is the pulse height response to an incident photon with a given phase space distribution defined by the chosen basis functions, F . The response function $R_{j,s}$ is directly estimated using a Monte Carlo method with incident flux as defined by the basis function F_j .

In order to construct an efficient response expansion method for pulse height tallies, it is necessary to identify a set of expansion bases F_j in Equation (8) to truncate the incident flux:

$$\varphi(\gamma^+) \approx \sum_{j=1}^M \sum_s \alpha_{j,s} F_j(\gamma_s^+), \quad (15)$$

so that the pulse height can be approximated as

$$r(\epsilon) \approx \sum_{j=1}^M \sum_s \alpha_{j,s} R_{j,s}(\epsilon). \quad (16)$$

The degree of truncation depends on the how well the expansion basis F approximates the incident flux. Additionally, a histogram representation of the response expansion can be approximated in a similar fashion shown in Equations (3-5) by substituting the pulse height for the response function $R_{j,s}(\epsilon)$.

The number of calculations for the response functions depends on the number of expansion functions, M , and S number of detector surfaces with a nonzero incident flux. For the case of a highly collimated detector, only one surface needs defining. Thus only M numbers of calculations are required to compute the response functions for the expansion method.

The IFRE method made use of Legendre polynomials for expanding the incident flux. In this method, Legendre polynomials are not used in expanding the energy dependence of the flux and instead a multigroup treatment is used. In general, Legendre polynomials are not a good choice for expanding the energy dependence of the

flux due to its sharp gradients. It is found that a significantly better choice is B-spline functions. Attention shall be directed towards the energy variable.

3.3 Incident Flux Approximation

B-splines are chosen as the basis for the incident flux expansion given in Equation (15). It is noted here that the incident flux is assumed mono-directional and constant in space and time. The incident flux $\varphi(\gamma_s^+)$ is written as $\varphi(E)$, where the other phase space variables are suppressed for clarity. Let the incident flux be defined on the interval $[E_0, E_L]$. The approximation is given by the following,

$$\varphi(E) \approx \varphi_k(E) = \sum_{j=1}^M \alpha_j B_{j,k}(E), \quad E_0 \leq E \leq E_L, \quad 1 \leq k \leq M, \quad (17)$$

where α_j are the coefficients [obtained using Equation (9)] of the M control points and $B_{j,k}$ are the normalized B-spline basis functions of order k . The k^{th} order B-spline basis functions form a set of degree $k - 1$ piecewise polynomials ($k - 2$ continuously differentiable) with breaks at $L + 1$ points in $[E_0, E_L]$ where $E_{l-1} \leq E_l$ ($l = 1, 2, \dots, L$). The number of control points, M , is a function of the number of points, L , and the order of B-splines, k . With $k - 2$ continuous derivatives on the interval defined by $L + 1$ points, the number of control points M is

$$M = L + k - 1. \quad (18)$$

The B-spline can be defined recursively by the Cox-de Boor recursion formulas [5]:

$$B_{j,1}(E) = \begin{cases} 1, & t_j \leq E \leq t_{j+1} \\ 0, & \text{otherwise} \end{cases}, \quad k = 1, \quad (19)$$

$$B_{j,k}(E) = \frac{E - t_j}{t_{j+k-1} - t_j} B_{j,k-1}(E) + \frac{t_{j+k} - E}{t_{j+k} - t_{j+1}} B_{j+1,k-1}(E), \quad 2 \leq k \leq M. \quad (20)$$

The elements t_j are referred to as knots and make up the knot vector. The knot vector determines the continuity and differentiability of the B-spline over a given interval

[6]. The only requirement of a knot vector is that the relation $t_j \leq t_{j+1}$ must be satisfied. Thus, a knot can have a multiplicity greater than one. A commonly used knot vector is the open knot vector which has multiplicity of knot values at the ends equal to the order k of the B-spline basis [5]. For the case of M control points, the knot vector can be defined as,

$$t_j = \begin{cases} E_0, & 1 \leq j \leq k \\ E_{j-k}, & k+1 \leq j \leq M \\ E_L, & M+1 \leq j \leq M+k \end{cases} . \quad (21)$$

An example of 1st, 2nd, and 3rd order B-spline basis set is shown in Figure 1 for the interval $[0, 1]$ with 5 evenly spaced breakpoints.

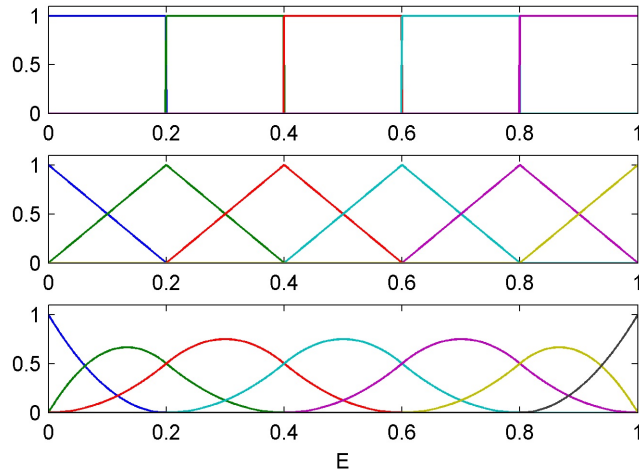


Figure 1: 1st (top), 2nd (middle) and 3rd (bottom) order B-spline basis on the interval $[0,1]$ with 5 uniform subintervals.

The following section describes the application of the B-splines in the response expansion method of section 3.2.

3.4 Implementation of the Method

Initially, a model of a detector of volume V is given in which fluxes are incident on the detector surfaces, s . From here, the B-spline basis knots and order are selected

based on whether the fluxes that will be incident on the detector are given as discrete in energy or continuous in energy. In the case of discrete in energy fluxes where energies are binned, a 1st order B-spline with knots located at the bin boundaries will provide an exact solution to the incident flux. For continuous flux cases, orders up to the 3rd usually suffice and knots are selected based on an understanding of the shape of the incident flux. For example, more knots are desired in energies where resonance peaks occur. In the continuous flux cases, the selection of the knots can have a much greater impact on the accuracy of the approximation than an increase in the B-spline order.

Once the knots and order of the B-spline are selected, a response function library is constructed using a modified version of MCNP5. The modifications allow for a continuous form of the B-spline to be applied as a boundary condition in MCNP5. Using the B-spline $B_{j,k}(E)$ as the boundary condition to Equations (10) and (11) for surface s of the detector, MCNP5 obtains the binned form of the solution to Equation (14). This is repeated over $j = 1, \dots, M$ for each surface s . Since the MCNP5 solutions of the response functions are in binned form, they are subsequently represented as histograms.

When constructing the response functions $R_{j,s}(E)$, it is important to note that MCNP5 will form a probability density function of the boundary condition prior to computation. Since the response functions $R_{j,s}(E)$ are computed separately, this means the total probability of each of the boundary conditions will be equal to one even though they only represent a fraction of the total probability. Thus, each response function is weighted according to the following equation:

$$\omega_i = \frac{t_{j+k} - t_j}{k(t_{M+k} - t_k)}. \quad (22)$$

Since MCNP5 forms probability density functions of the boundary conditions prior to computation, the probability density function of a given incident flux is computed. The incident flux is then approximated as a set of B-splines. The coefficients of

the B-spline approximation can be computed by solving a least squares fit utilizing Equation (9). The linear combination of the products of the incident flux coefficients and the weighted response functions are computed to obtain the solution to the pulse height tally. Chapter IV provides some examples utilizing the method.

CHAPTER IV

RESULTS

For validation of the energy dependent B-spline PHRE method, several flux spectra are employed as incident fluxes on a detector surface/window. To demonstrate the accuracy and applicability of the method for both deterministic and stochastic incident fluxes, discrete and continuous in energy incident fluxes are used.

4.1 Method Verification

A simple model is constructed for the purpose of verifying the response expansion method. The model is a 13.5x13.5x7.62 cm CsI(Na) crystal in which photon fluxes are incident on one of the 13.5x13.5 cm detector faces. The incident fluxes are energy dependent, mono-directional (e.g., highly collimated), spatially uniform, time independent, and are defined on the interval [0, 20 MeV] as either discrete (multigroup, see Appendix A for energy grouping), or continuous in energy.

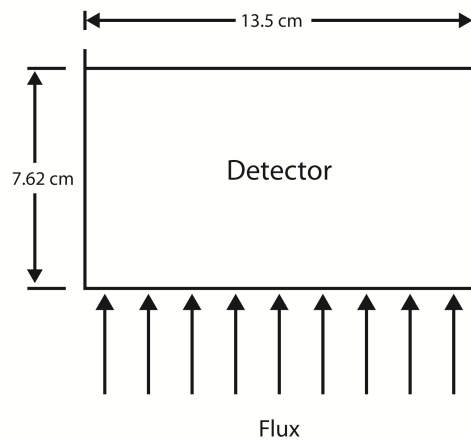


Figure 2: Diagram of the detector with a photon flux incident on one of the 13.5x13.5 cm detector faces. The detector is composed of a CsI(Na) crystal.

4.1.1 Multigroup Flux Approximations

The multigroup incident fluxes are represented as histograms. From Equation (19), it can be seen that the first order B-spline approximation is equivalent to histogram approximations. Thus, first order B-splines with knots located at the bin boundaries are used in approximating the pulse height tallies for the multigroup fluxes.

The following figures show the two multigroup fluxes used for verification of the response expansion method. The first represents the flux from a cargo container homogenously filled with air and the second with third-density water. These two fluxes are similar to those found in active interrogation scenarios, where deterministic methods are used to solve for the incident fluxes.

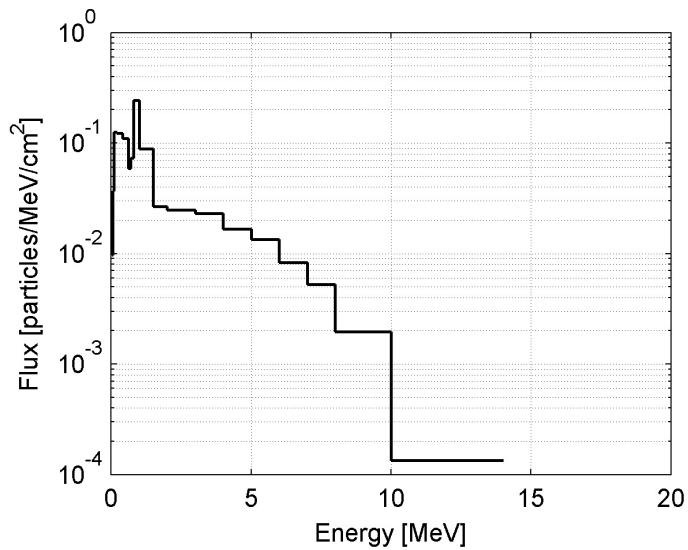


Figure 3: Incident flux from an air cargo

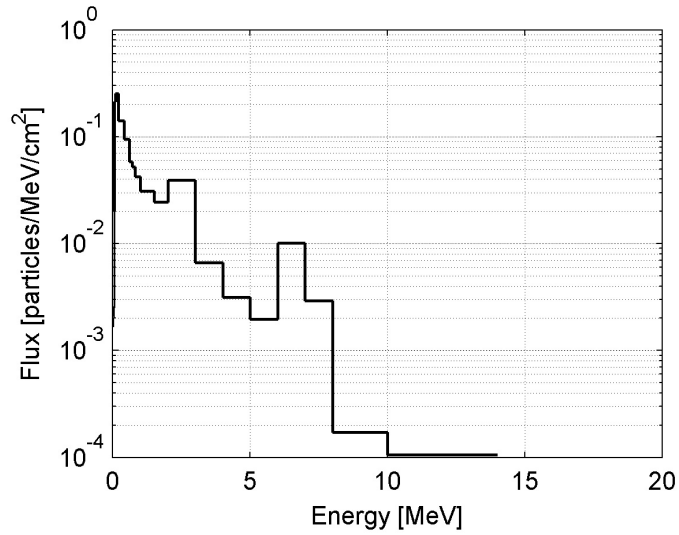


Figure 4: Incident flux from a third-density water cargo

4.1.2 Continuous Flux Approximations

An analytical form of a U-235 prompt fission gamma spectrum is used for the continuous flux spectrum. The energy spectrum of the prompt fission gamma rays for U-235 can be given by the following probability function [7]:

$$N(E) = \begin{cases} 38.13(E - 0.085)e^{1.648E}, & 0.085 < E < 0.3\text{MeV} \\ 26.8e^{-2.30E}, & 0.3 < E < 1.0\text{MeV} \\ 8.0e^{-1.10E}, & 1.0 < E < 8.0\text{MeV} \end{cases} . \quad (23)$$

The 1st, 2nd, and 3rd order B-spline curves with knots located at the bin boundaries (see Appendix A) are used to approximate the spectrum. Figure 5 shows the approximations in comparison to the exact spectrum. The approximations were performed using the least squares method of Equation (9).

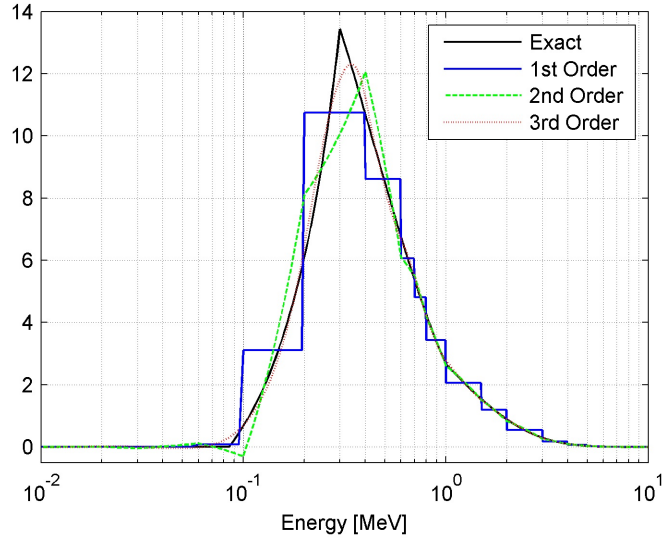


Figure 5: The 1st, 2nd and 3rd order B-spline approximations of the U-235 prompt fission gamma distribution compared to the exact solution of the distribution.

To improve the goodness-of-fit, the multiplicity of the knots located at the discontinuities 0.3 MeV and 1.00 MeV of Equation (23) are set to one for the 2nd order approximation and two for the 3rd order approximation. Figure 6 shows the improvements made as a result of the additional knots.

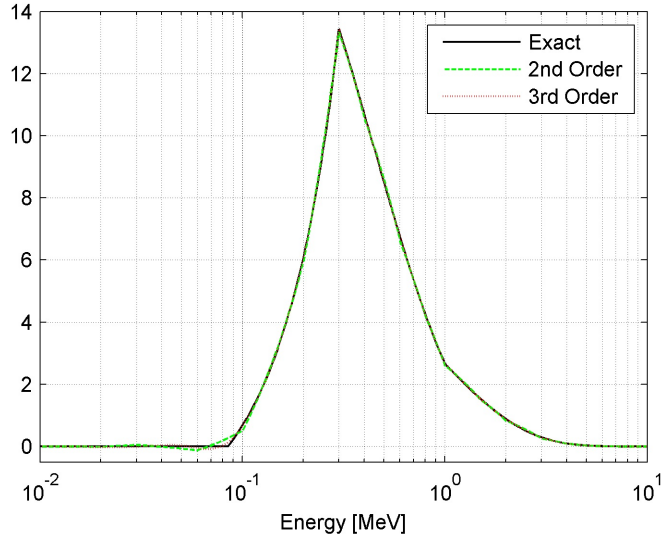


Figure 6: The 2^{nd} and 3^{rd} order B-spline approximations, with additional knots at 0.3 MeV and 1.0 MeV, of the U-235 prompt fission gamma distribution compared to the exact solution of the distribution.

For the least squares fits, the 2-norm of the difference between the B-spline approximations and the exact solution, which corresponds to the Euclidean distance between the two, is used to determine the goodness-of-fit:

$$\left(\int_E |\varphi_k(E) - \varphi(E)|^2 \right)^{\frac{1}{2}}. \quad (24)$$

Smaller 2-norm values correspond to better fits, where the smallest value is zero (which is equivalent to an exact fit). Table 1 shows the 2-norms for the approximations.

Table 1: 2-Norms of U-235 flux distribution for B-spline approximations

Order	2-Norm
1 st	17.52
2 nd	12.67
3 rd	4.60
2 nd (added knots)	1.05
3 rd (added knots)	0.25

Approximations beyond 3rd orders provide little improvement to estimate the flux spectrum.

4.1.3 Pulse Height Tally Solutions

The response functions for the response expansion method are computed using a modified version of MCNP5. The modifications allow for the B-spline basis functions to be input as continuous functions. The B-spline bases used to approximate the multigroup and continuous cases of the incident fluxes are utilized to construct the response functions over the interval [0, 20 MeV], with 0.2 MeV binning. Coefficients of the B-spline approximations of the incident fluxes are obtained. The pulse height tally is then constructed from the linear combination of the coefficients and the response functions. The response expansion method's solutions of the detector pulse height tally are compared to those directly obtained from MCNP5. The MCNP5 solutions were computed using the incident fluxes as the boundary conditions to the detector over the same interval and binning used to construct the response function. Solutions using MCNP5 were well converged, with average relative standard deviations $\left[\frac{\sum_{i=1}^N \sigma_i}{\sum_{i=1}^N r(\epsilon_i)} \right]$ of 0.1%.

Figure 7 shows the response expansion method and MCNP5 pulse height tally solutions associated with the incident flux from the air cargo (left plot), with an error analysis plot that compares the absolute differences of the two methods against their standard deviations (right plot). As seen by the standard deviations of the

response expansion method, σ_{RM} , and MCNP5's standard deviations, σ_{MCNP5} , the response expansion method's results are found to be better converged than that of MCNP5 with the response expansion method's average relative standard deviation of 0.03%. Resulting from the better convergence of the response expansion method, the standard deviation of the absolute differences, $\sigma_{MCNP5-RM}$, is mainly dominated by σ_{MCNP5} . Comparing $\sigma_{MCNP5-RM}$ to the absolute differences of the two methods, it can be seen that the differences between the two methods can be mainly attributed to statistical uncertainty. The same arguments above apply for the pulse height tally solutions associated with the incident flux from the third-density water cargo shown in Figure 8. The average relative standard deviation of the response expansion method for the pulse height tally from the third-density water cargo was also 0.03%.

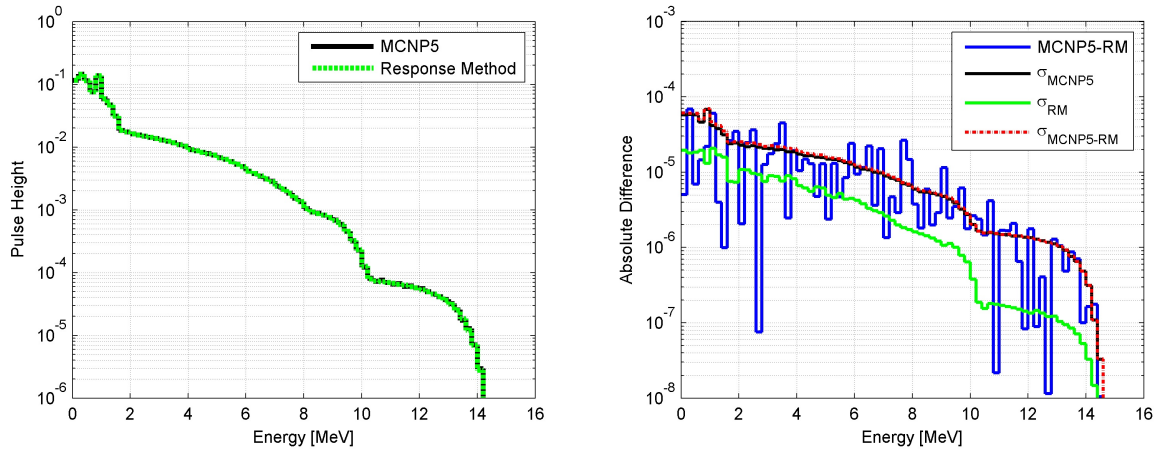


Figure 7: Comparison of MCNP5's and the response expansion method's pulse height tally associated with the incident flux from the air cargo.

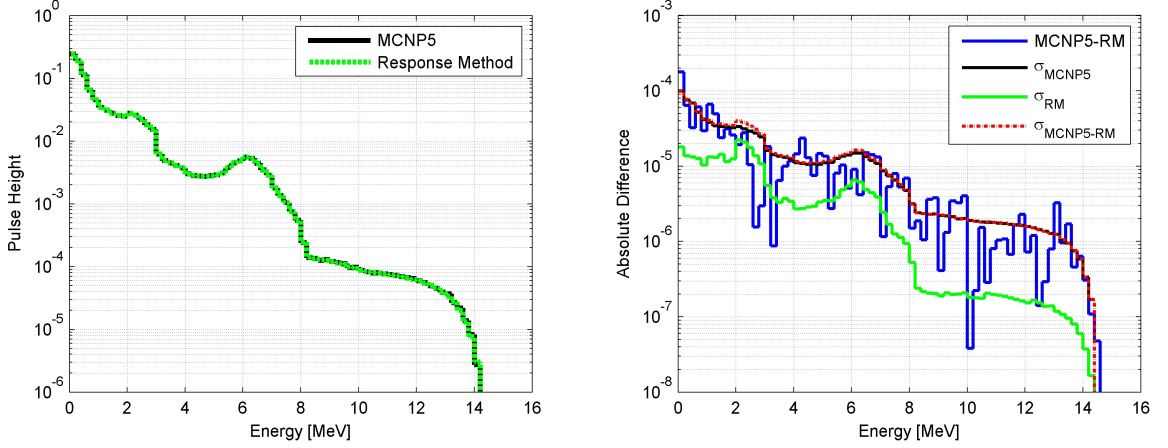


Figure 8: Comparison of MCNP5's and the response expansion method's pulse height tally associated with the incident flux from the third-density water cargo.

For the case of the 1st order B-spline approximation of the U-235 prompt fission gamma distribution, the absolute differences of the response expansion method and MCNP5 solutions were roughly an order of magnitude higher than $\sigma_{MCNP5-RM}$, as can be seen in Figure 9. The difference between the absolute difference and $\sigma_{MCNP5-RM}$ is attributed to the differences between the approximated and exact incident flux. Again, as in the multigroup flux cases, the $\sigma_{MCNP5-RM}$ is dominated by σ_{MCNP5} , more so than the multigroup flux cases as the average relative standard deviation of the response expansion method using the 1st order B-spline approximation is 0.004%. The remainder of the approximations (2nd and 3rd with and without added knots) of the U-235 example had average relative standard deviations of 0.005%.

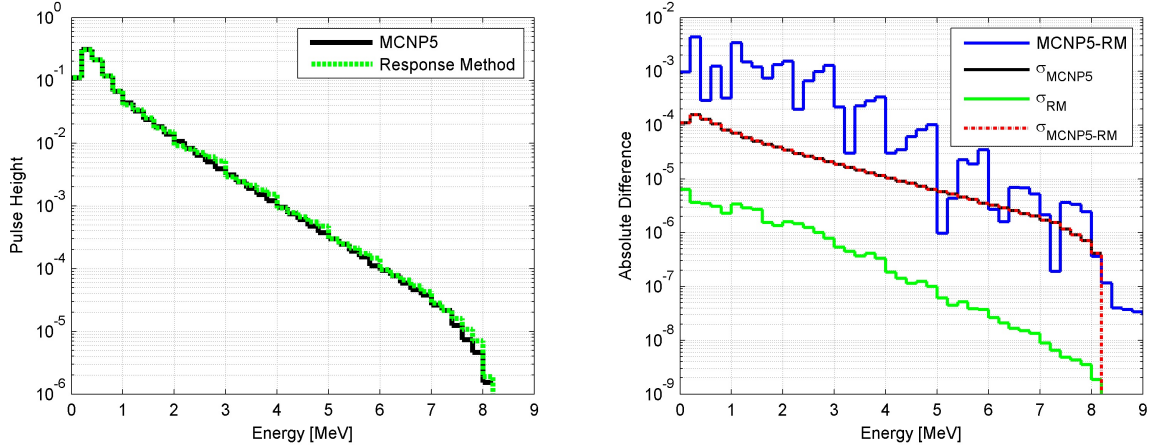


Figure 9: Comparison of the pulse height tally associated with the U-235 distribution from MCNP5 and the pulse height tally from the response expansion method using the 1st order B-spline approximation of the U-235 distribution.

The 2nd order B-spline approximation is shown in Figure 10. Again as in the 1st order approximation, the difference in the approximation compared to the exact incident flux results adds additional error to the response expansion method solutions. The largest difference can be seen in the range 0 to 1 MeV. This is associated with the approximation's difficulty in capturing the peak at 0.3 MeV. Going to the 3rd order B-spline approximation made significant improvements to the response expansion method's solution within this range as can be seen in Figure 11.

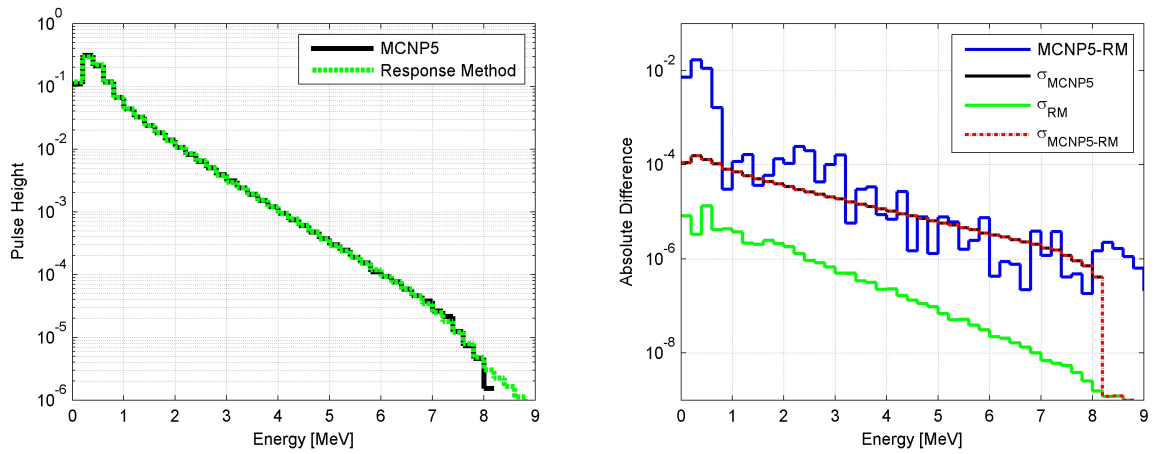


Figure 10: Comparison of the pulse height tally associated with the U-235 distribution from MCNP5 and the pulse height tally from the response expansion method using the 2^{nd} order B-spline approximation of the U-235 distribution.

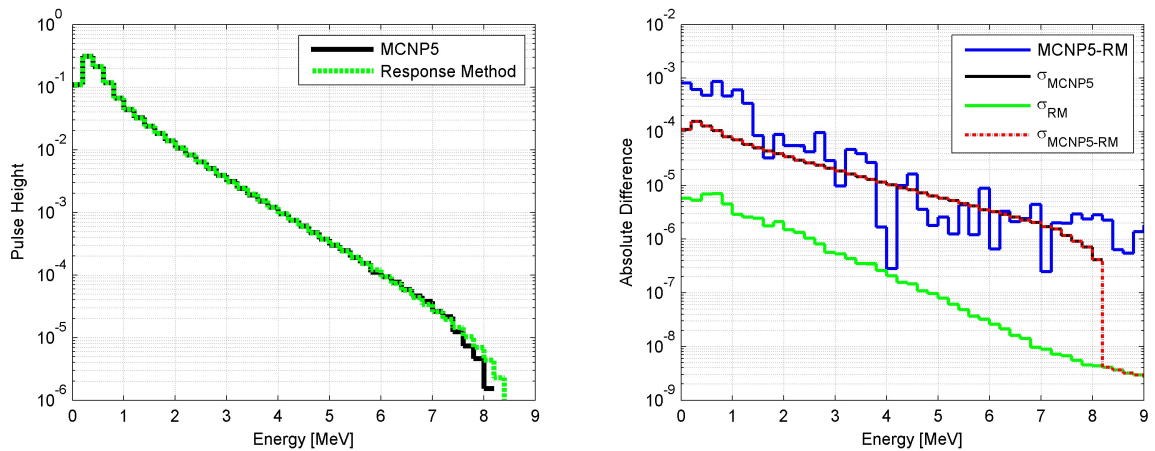


Figure 11: Comparison of the pulse height tally associated with the U-235 distribution from MCNP5 and the pulse height tally from the response expansion method using the 3^{rd} order B-spline approximation of the U-235 distribution.

For the 2^{nd} and 3^{rd} order B-spline approximations with additional knots, further improvements were made to the response expansion method solutions of the U-235 spectrum. The absolute differences between the response expansion method and MCNP5 were reduced to within the same magnitude as that of $\sigma_{MCNP5-RM}$. This can be seen in Figures 12 and 13 for the 2^{nd} and 3^{rd} order B-spline approximations with additional knots.

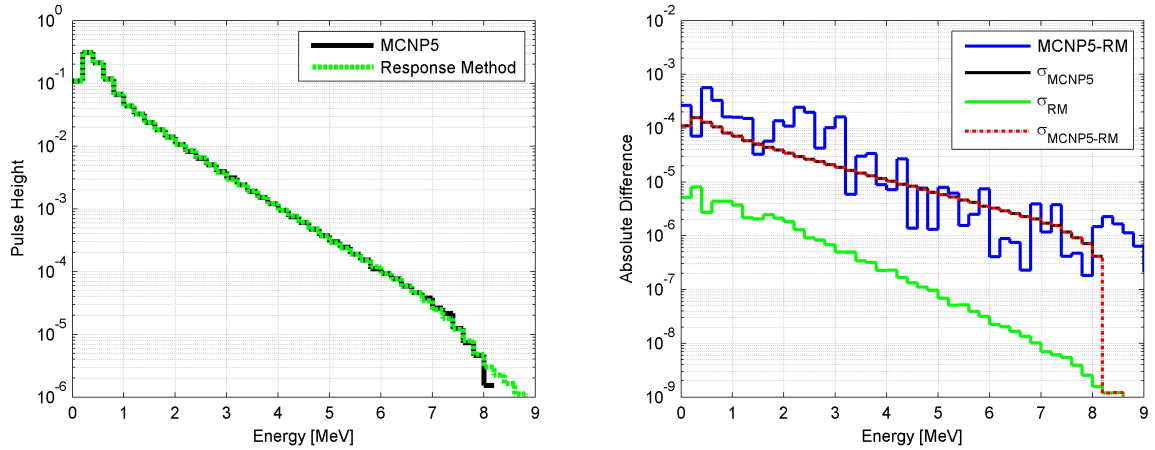


Figure 12: Comparison of the pulse height tally associated with the U-235 distribution from MCNP5 and the pulse height tally from the response expansion method using the 2^{nd} order B-spline approximation (with additional knots) of the U-235 distribution.

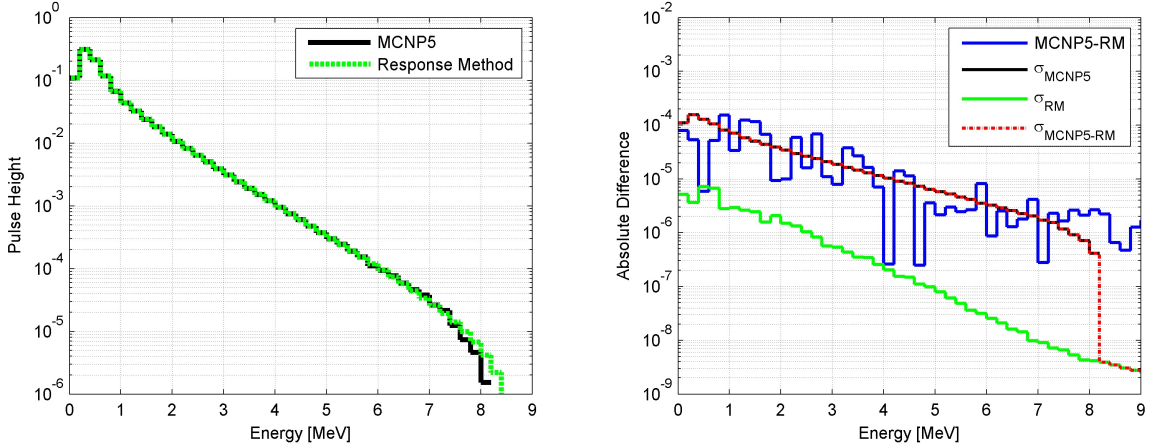


Figure 13: Comparison of the pulse height tally associated with the U-235 distribution from MCNP5 and the pulse height tally from the response expansion method using the 3rd order B-spline approximation (with additional knots) of the U-235 distribution.

4.2 Accuracy and Efficiency

For comparison of the response expansion method to MCNP5, the following is used:

$$e_1 = \frac{\|r_k - r_{MCNP5}\|_1}{\|r_{MCNP5}\|_1}, \quad (25)$$

where $\|\cdot\|_1$ is the 1-norm of the values within. For a set of values, the 1-norm is equivalent to the sum of their absolute values [4]. The value e_1 is equivalent to the mean weighted error,

$$\frac{\sum_{i=1}^N |RE| \cdot r_{MCNP5}(\epsilon_i)}{N \cdot \bar{r}_{MCNP5}}, \quad (26)$$

where,

$$RE = \frac{r_k(\epsilon_i) - r_{MCNP5}(\epsilon_i)}{r_{MCNP5}(\epsilon_i)}, \quad (27)$$

which places more importance on larger values than on those nearest zero. Since the pulse height tallies encompass several orders of magnitude, this is a very good method of comparison. The mean weighted errors for the response expansion solutions of the pulse height tallies with error associated with standard deviations (1σ) are shown in Table 2.

Table 2: Percent mean weighted errors of response expansion method for pulse height tallies

Pulse Height Tally	Percent Mean Weighted Error				
	1 st Order	2 nd Order	3 rd Order	2 nd Order (added knots)	3 rd Order (added knots)
Air cargo	0.07 ± 0.02	-	-	-	-
Third-density water cargo	0.09 ± 0.02	-	-	-	-
U-235	2.16 ± 0.03	3.83 ± 0.03	0.49 ± 0.03	0.29 ± 0.03	0.10 ± 0.03

Computation times for each of the response functions were set to 5000 minutes to reduce standard deviations to a nominal level. Table 3 shows the computation times for the response expansion method (excluding the response function computation times), as compared to MCNP5 calculations where the average relative standard deviation was used to obtain similar statistical precision. Computation times for the U-235 using the response expansion method are longer due to the least squares fitting for the flux approximation.

Table 3: Computation times for pulse height tally solutions for MCNP5 and the response expansion method

Pulse Height Tally	Computation Times					
	MCNP5 <i>Average Relative Standard Deviation</i>	Response Method				
		1 st Order	2 nd Order	3 rd Order	2 nd Order (added knots)	3 rd Order (added knots)
Air cargo	451 min <i>0.0010</i>	0.01 sec	-	-	-	-
Third-density water cargo	665 min <i>0.0010</i>	0.01 sec	-	-	-	-
U-235	141 min <i>0.0010</i>	0.34 sec	0.35 sec	0.36 sec	0.37 sec	0.38 sec

Note that the run time of the direct Monte Carlo calculations is significantly underestimated (by a factor of 9). The direct Monte Carlo results presented in table 3 have a statistical uncertainty 3 times larger than the response expansion method.

CHAPTER V

CONCLUSION, RECOMMENDATION, AND FUTURE WORK

A new pulse height tally response expansion method has been developed. The method uses a library of precomputed response functions that depend on the geometry and composition of the detector. Provided the incident flux, the library is used to construct a pulse height tally on-the-fly. The method's accuracy and efficiency were evaluated for both discrete in energy and continuous in energy incident fluxes. Pulse height tallies computed using the response expansion method were in excellent agreement to MCNP5, having mean weighted errors around 0.1 percent. To reduce the mean weighted error to 0.1 percent for the continuous flux approximations, the 3rd order spline with additional knots was needed. The addition of knots and increase in order had little impact on the computation time of the pulse height tally. The method is computationally 4-6 orders of magnitude faster than MCNP5.

Response functions can take a substantial amount of time to compute. However, they are calculated in a precomputation phase and serve as a library for future calculations of detector responses. Thus, computation of response functions does not affect the detector response calculation times and computing detector responses take a fraction of a second.

A direct application of the response expansion method is to interrogation problems. These types of problems usually consist of a radiation detector and a container with an assortment of materials to be identified via the emission of particles. In active interrogation, a source is also present and is incident on the container to improve identification of materials with normally low particle emissions. Such problems could

include interrogation of conventional explosives or cargo containers with special nuclear materials. To rapidly simulate interrogation problems, the source and container would normally be modeled by a deterministic method to obtain the angular flux incident on the detector window. For the detector, the response expansion method is used to generate the detector's response. Thus, the angular flux incident on the detector boundaries together with a pre-computed library of response functions is used to generate the detector's response on-the-fly.

The incident fluxes in this study were assumed uniform in space and mono-directional in angle. Additional work is required to expand this method in modeling the incident flux in its full phase space (i.e. angular and spatial variables).

APPENDIX A

FLUX ENERGY BINS

Table 4: Energy bins for flux spectrums

Energy Bins (MeV)
0.00
0.02
0.03
0.06
0.10
0.20
0.40
0.60
0.70
0.80
1.00
1.50
2.00
3.00
4.00
5.00
6.00
7.00
8.00
10.0
14.0
20.0

REFERENCES

- [1] M. W. Shaver, L. E. Smith, R. T. Pagh, E. A. Miller, and R. S. Wittman, “The Coupling of a Deterministic Transport Field Solution to a Monte Carlo Boundary Condition for the Simulation of Large Gamma-Ray Spectrometers,” *Nuclear Technology*, vol. 168, pp. 95–100, October 2009.
- [2] J. Benz and T. Palmer, “Pulse Height Distributions from Deterministic Radiation Transport Simulations,” *Annals of Nuclear Energy*, vol. 37, pp. 1486–1493, 2010.
- [3] S. Mosher and F. Rahnema, “The Incident Flux Response Expansion Method for Heterogeneous Coarse Mesh Transport Problems,” *Transport Theory and Statistical Physics*, vol. 24, pp. 1–26, 2006.
- [4] L. N. Trefethen and I. D. Bau, *Numerical Linear Algebra*. Siam, 1997.
- [5] C. Boor, *A Practical Guide to Splines, Revised Edition*. Springer-Verlag New York, Inc., 2001.
- [6] D. F. Rogers, *An Introduction to NURBS With Historical Perspective*. Academic Press, 2001.
- [7] J. M. Verbeke, C. Hagmann, and D. Wright, “Simulation of Neutron and Gamma Ray Emission from Fission and Photofission,” *UCRL-AR-228518*, May 2010.
- [8] “MCNP - A General Monte Carlo N-Particle Transport Code, Version 5,” *LA-UR-03-1987*, 2003.